

## Strong Neutron- $\gamma$ Competition above the Neutron Threshold in the Decay of $^{70}\text{Co}$

A. Spyrou,<sup>1,2,3,\*</sup> S. N. Liddick,<sup>1,4,3</sup> F. Naqvi,<sup>1,3</sup> B. P. Crider,<sup>1</sup> A. C. Dombos,<sup>1,2,3</sup> D. L. Bleuel,<sup>5</sup> B. A. Brown,<sup>1,2,3</sup> A. Couture,<sup>6</sup> L. Crespo Campo,<sup>7</sup> M. Guttormsen,<sup>7</sup> A. C. Larsen,<sup>7</sup> R. Lewis,<sup>1,4</sup> P. Möller,<sup>6</sup> S. Mosby,<sup>6</sup> M. R. Mumpower,<sup>6</sup> G. Perdikakis,<sup>8,1,3</sup> C. J. Prokop,<sup>1,4</sup> T. Renström,<sup>7</sup> S. Siem,<sup>7</sup> S. J. Quinn,<sup>1,2,3</sup> and S. Valenta<sup>9</sup>

<sup>1</sup>National Superconducting Cyclotron Laboratory, Michigan State University, East Lansing, Michigan 48824, USA

<sup>2</sup>Department of Physics and Astronomy, Michigan State University, East Lansing, Michigan 48824, USA

<sup>3</sup>Joint Institute for Nuclear Astrophysics, Michigan State University, East Lansing, Michigan 48824, USA

<sup>4</sup>Department of Chemistry, Michigan State University, East Lansing, Michigan 48824, USA

<sup>5</sup>Lawrence Livermore National Laboratory, 7000 East Avenue, Livermore, California 94550-9234, USA

<sup>6</sup>Los Alamos National Laboratory, Los Alamos, New Mexico 87545, USA

<sup>7</sup>Department of Physics, University of Oslo, NO-0316 Oslo, Norway

<sup>8</sup>Central Michigan University, Mt. Pleasant, Michigan 48859, USA

<sup>9</sup>Faculty of Mathematics and Physics, Charles University in Prague, V Holešovičkách 2,

CZ-180 00 Prague 8, Czech Republic

(Received 18 May 2016; published 29 September 2016)

The  $\beta$ -decay intensity of  $^{70}\text{Co}$  was measured for the first time using the technique of total absorption spectroscopy. The large  $\beta$ -decay  $Q$  value [12.3(3) MeV] offers a rare opportunity to study  $\beta$ -decay properties in a broad energy range. Two surprising features were observed in the experimental results, namely, the large fragmentation of the  $\beta$  intensity at high energies, as well as the strong competition between  $\gamma$  rays and neutrons, up to more than 2 MeV above the neutron-separation energy. The data are compared to two theoretical calculations: the shell model and the quasiparticle random phase approximation (QRPA). Both models seem to be missing a significant strength at high excitation energies. Possible interpretations of this discrepancy are discussed. The shell model is used for a detailed nuclear structure interpretation and helps to explain the observed  $\gamma$ -neutron competition. The comparison to the QRPA calculations is done as a means to test a model that provides global  $\beta$ -decay properties for astrophysical calculations. Our work demonstrates the importance of performing detailed comparisons to experimental results, beyond the simple half-life comparisons. A realistic and robust description of the  $\beta$ -decay intensity is crucial for our understanding of nuclear structure as well as of  $r$ -process nucleosynthesis.

DOI: 10.1103/PhysRevLett.117.142701

The connections between the microcosmos of nuclear structure and the macrocosmos of stellar phenomena are among the most elegant features of the field of nuclear astrophysics. Unexpected changes in nuclear structure while moving away from the well-known stable isotopes can alter the calculated abundance distributions. It is therefore critical to understand not only the evolution of nuclear structure itself but also the implications it has to astrophysical calculations.

It is well known today that roughly half of the isotopes of the heavy elements are produced in the rapid neutron-capture process ( $r$  process). Despite six decades of study [1,2], the astrophysical site for the  $r$  process remains elusive. Various plausible scenarios have been proposed [3,4], with the most dominant being core-collapse supernovae, e.g., Refs. [5–8], and neutron-star mergers, e.g., Refs. [9,10]. Many astrophysical observations are designed to answer this important question, and the most recent advancement is the observation of dwarf spheroidal galaxies [11], which were found consistent with  $r$ -process nucleosynthesis from rare events. On the other hand, the nuclear input in  $r$ -process models is also highly uncertain,

and the present Letter focuses on an effort to understand the nuclear structure input, in particular, for light  $r$ -process elements, where evidence suggests a production mechanism possibly different from the heavier ones [3,12].

$r$ -process sensitivity studies show that nuclear masses, neutron-capture rates, and  $\beta$ -decay properties such as half-lives ( $T_{1/2}$ ) and  $\beta$ -delayed neutron-emission probabilities ( $P_n$ ) all have a large impact on the final abundance distribution [13,14]. Experiments have long attempted to provide measurements of the masses and  $\beta$ -decay properties for as many nuclei as possible, e.g., most recently [15–17]. The study of neutron-capture reactions is much more challenging experimentally, and indirect techniques are being developed for constraining the reaction rates [18–22].

On top of the extended experimental efforts to provide data for  $r$ -process calculations, reliable theoretical calculations are necessary for the isotopes that are out of reach by current facilities. It is therefore critical to test these theoretical models as extensively as possible. For  $\beta$ -decay properties, the quasiparticle random phase approximation (QRPA) is commonly used to provide global predictions across the nuclear chart [23–25]. Typically, the calculations

are tested against known half-lives and  $\beta$ -delayed neutron-emission probabilities. However, these quantities are calculated from the  $\beta$ -decay intensity  $I_\beta$  or the Gamow-Teller strength  $B(\text{GT})$  distributions, and a more sensitive test of the theory is the direct comparison to experimental  $I_\beta$  and extracted  $B(\text{GT})$ .

Experimentally, the measurement of the  $I_\beta$  and  $B(\text{GT})$  is commonly done either via  $\beta$ -decay measurements or through charge-exchange reaction measurements [26,27]. Although the latter can provide the  $B(\text{GT})$  in a larger energy region, as a reaction-based technique, it is limited to nuclei relatively close to the valley of  $\beta$  stability.  $\beta$ -decay studies can be extended farther from stability into regions that are directly relevant to the  $r$  process; however, they are limited by the  $\beta$ -decay  $Q$  value. In the present Letter, we present the first measurement of  $I_\beta$  for the case of  $^{70}\text{Co}$ , an isotope with a very large  $\beta$ -decay  $Q$  value [12.3(3) MeV [28]], which offers a unique opportunity to compare to theoretical calculations, both far from stability and within a wide energy window.

$^{70}\text{Co}$  decays into  $^{70}\text{Ni}$ , a nucleus with magic proton number  $Z = 28$  and two neutrons from the semimagic neutron number  $N = 40$ . Nuclei in this region are considered to be dominated by near-spherical features [29]; however, shape coexistence has been observed in some isotopes [30–35]. In particular,  $^{70}\text{Co}$  is known to have two  $\beta$ -decaying isomeric states, a high-spin one ( $6^-, 7^-$ ) with short half-life ( $\approx 110$  ms [34,36–39]) and a low-spin one ( $3^+$ ) with a longer half-life ( $\approx 500$  ms [34,37]), which are believed to have different shapes. In the present Letter, we only observe the high-spin state, which is considered near spherical.

The experiment was performed at the National Superconducting Cyclotron Laboratory (NSCL), at Michigan State University. A primary beam of  $^{86}\text{Kr}$  at 140 MeV/nucleon was impinged on a  $^9\text{Be}$  target, and the fragmentation reaction products were separated in flight using the A1900 fragment separator [40] and delivered to the experimental setup. The setup was presented in Ref. [41], and briefly it consisted of a series of silicon detectors for beam identification and implantation, as well as the Summing NaI (SuN) detector [42] for  $\gamma$ -ray detection. SuN is a large-volume NaI(Tl) detector, with eight optically isolated segments. A double-sided silicon-strip detector (DSSD) was used to detect both the implanted ions and the subsequent  $\beta$ -decay electrons and correlate them in time.

The technique used for the extraction of  $I_\beta$  is the technique of total absorption spectroscopy (TAS) [27]. TAS was introduced four decades ago as a solution to the so-called ‘‘pandemonium effect’’ [43], which is a term used to describe the incorrect extraction of  $\beta$ -decay intensity when using a low-efficiency  $\gamma$ -ray detector. When the detector has efficiency close to 100%, the energy of individual  $\gamma$  rays in a cascade can be summed, and the initial excitation energy correctly identified. In the present

experiment, the TAS technique was applied for the first time to study the  $\beta$  decay of  $^{70}\text{Co}$ .

Unlike previous experiments, where the long-lived  $\beta$ -decaying isomeric state was also observed [34,37], in the present experiment no signature of this low-spin state was found. This was evident in the decay time of  $^{70}\text{Co}$ , which was consistent with the half-life of the short-lived state, and also by the nonobservation of  $\gamma$  rays at 1866 keV, coming from a  $2^+$  state that is strongly populated in the decay of the long-lived state [34,37]. The low-lying energy levels and  $\gamma$  decays of Ref. [34] were confirmed up to  $\approx 4$  MeV.

For the extraction of the  $\beta$ -decay intensity, three experimental spectra were used (Fig. 1). (1) The event-by-event energy sum of all segments in SuN to produce the total absorption spectrum. This spectrum is sensitive to the initial excitation energy populated in  $\beta$  decay. (2) The individual spectra of the eight segments of SuN. These are sensitive to the individual  $\gamma$  rays that participate in the cascade. (3) The number of segments that record a signal within an event (multiplicity). This spectrum is sensitive to the  $\gamma$  multiplicity in a cascade. A random ion- $\beta$  correlation was used to produce

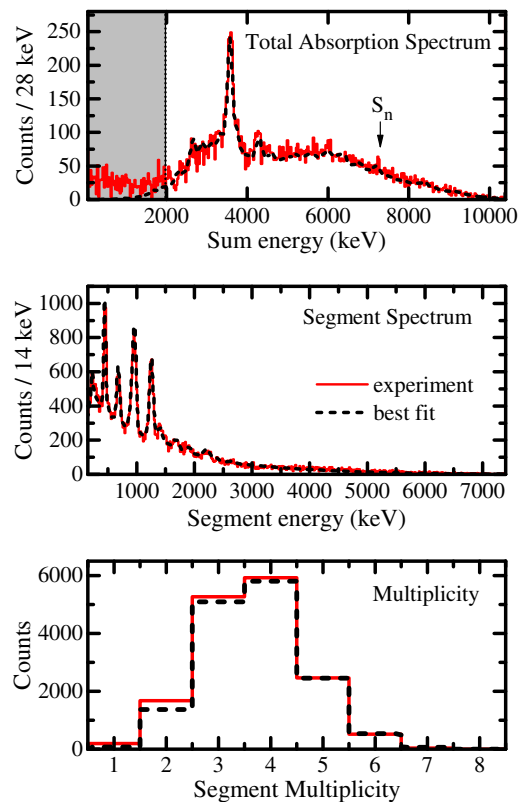


FIG. 1. Experimental spectra for the decay of  $^{70}\text{Co}$  (solid red line) together with the best fit of the  $\chi^2$  minimization analysis procedure (dashed black line). The top panel shows the TAS spectrum, the middle panel shows the segment spectrum, and the bottom panel shows the segment multiplicity in the SuN detector. All experimental spectra are gated on implanted  $^{70}\text{Co}$  ions, and the random correlation background was subtracted.

“background” SuN spectra and was subtracted from the “true” ion- $\beta$ -correlation spectra [44,45].

The low-energy part of the  $^{70}\text{Ni}$  level scheme from Ref. [34], up to  $\approx 4$  MeV, was used as input in a well-characterized GEANT4 simulation [42] of SuN. Above that energy, the level scheme is not known, and “artificial” cascades were produced using the statistical model code DICEBOX [46]. Assuming that the ground state spin and parity of  $^{70}\text{Co}$  is  $6^-$  (the results do not change if the alternative spin assignment of  $7^-$  is used),  $\beta$  decay is expected to dominantly populate states with spin and parity  $5^-$ ,  $6^-$ , and  $7^-$ . These were the spins assumed as entry states in DICEBOX. Artificial entry states for each of the three spins were created every 200 keV. Although in reality we expect more than one level in the 200 keV window, these would not be resolved due to the energy resolution of SuN. Therefore, the extracted  $I_\beta$  corresponds to the feeding of each energy window and not individual levels. For each entry state, random deexcitation paths were produced in DICEBOX and fed into the GEANT4 simulation. Using this simulation process, three spectra were produced by GEANT4 for each entry state: the TAS spectrum, the segment spectrum, and multiplicity. These simulated spectra were used to perform a  $\chi^2$  minimization, fitting all three experimental spectra simultaneously, with the  $I_\beta$  to each entry state as free parameters. The best fit from this analysis is shown in Fig. 1. An overall excellent agreement with the experimental spectra is observed. It should be noted that at low energies, the TAS spectrum is dominated by significant statistical fluctuations coming from the subtraction of random correlations. As there are no levels in  $^{70}\text{Ni}$  expected to be populated in the observed decay, the region below 2 MeV was excluded from the  $\chi^2$  fit. The upper limit for the TAS spectrum was at 10.4 MeV, above which there was no significant population.

While the TAS spectrum exhibits a strong population of a level at 3592 keV, as seen in previous experiments [34,35], it also presents two additional surprising features: strong population of high energy levels in what looks like a continuous distribution and strong  $\gamma$ -ray emission above the neutron-separation energy at 7.3 MeV [28]. These two features will be discussed in the following, through the comparison to theoretical calculations.

The best fit of the experimental spectra shown in Fig. 1 resulted in the cumulative  $\beta$ -decay intensity of Fig. 2 (black line), together with the experimental uncertainties (green-shaded area). The uncertainty band is dominated by the statistical uncertainty of the TAS spectrum ( $\approx 15\%$  up to 8 MeV, which gradually increases at higher energies and reaches 50% at 10 MeV). A  $\approx 10\%$  uncertainty in SuN’s efficiency [42] was also included. An additional uncertainty, not included in the figure, comes from the unknown  $\beta$ -delayed neutron-emission probability. A recent experiment at NSCL using a high resolution  $\gamma$ -detection system [34,47] searched for  $\gamma$ -ray emission from excited states in  $^{69}\text{Ni}$  which are populated via  $\beta$ -delayed neutron emission

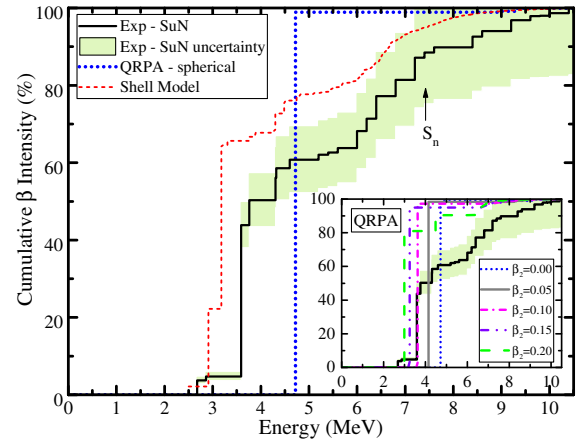


FIG. 2. Cumulative  $\beta$ -decay intensity of  $^{70}\text{Co}$  versus excitation energy of the final states in  $^{70}\text{Ni}$ . The solid black line and green-shaded area are the experimental results with uncertainties. The dashed red line is a shell-model calculation (see the text for details). The thick dotted blue line is a QRPA calculation under the assumption of spherical shape. The inset shows QRPA calculations under different deformation assumptions.

from  $^{70}\text{Co}$ . No  $\gamma$  rays were observed from the decay of the high-spin state in  $^{70}\text{Co}$ , while for the low-spin state a  $P_n$  of 3.5% was extracted. This “nonobservation” of neutron emission for the state of interest does not exclude the possibility of neutron emission, populating directly the ground state of  $^{69}\text{Ni}$ . Nevertheless, the conclusions of the present work will not be significantly affected by a small percentage of  $P_n$ , within the aforementioned remaining uncertainties.

In Fig. 2, the experimental  $\beta$ -decay intensity is compared to two theoretical calculations: The dotted blue line corresponds to a calculation using the QRPA approach in the folded-Yukawa QRPA model [25] under the assumption of spherical shape [29]. The dashed red line corresponds to a shell-model calculation carried out in the  $0f_{7/2}, 0f_{5/2}, 1p_{3/2}, 1p_{1/2}, 0g_{9/2}, 0g_{7/2}$  model space. We used the GPFX1A Hamiltonian [48] for the  $0f$ - $1p$  part of this model space. The part of the Hamiltonian involving the  $0g$  orbitals was obtained from the  $N^3\text{LO}$  interaction [49] renormalized by  $V_{\text{lowk}}$  into six major oscillator shells and then renormalized up to second order perturbation theory into the model space [50]. The single-particle energies were determined from the low-lying spectra and relative binding energies of  $^{69,70}\text{Ni}$ ,  $^{69}\text{Co}$ , and  $^{71}\text{Cu}$ . The spin-orbit spacings for  $0f_{7/2} - 0f_{5/2}$  and  $0g_{9/2} - 0g_{7/2}$  were set to about 6 MeV. Starting with a  $0f_{7/2}$  proton closed-shell configuration, the lowest  $5^-$  proton particle-hole state in  $^{70}\text{Ni}$  comes at about 7.5 MeV. The initial  $^{70}\text{Co}$   $6^-$  state was taken to have the configuration  $C(\nu 0g_{9/2})^3(\pi 0f_{7/2})^{-1}$ , where  $C$  is the closed-shell configuration  $(\nu 0f_{5/2})^6(\nu 1p_{3/2})^4(\nu 1p_{1/2})^2(\pi 0f_{7/2})^8$ . The  $^{70}\text{Ni}$  final states were obtained from all possible configurations for one-particle–one-hole ( $1p - 1h$ ) excitations relative to

$^{70}\text{Co}$ , about 12 000 final states. These final states were needed to obtain the Gamow-Teller sum-rule strength of  $3(N - Z) = 48$ .

The cumulative  $\beta$ -decay intensity of Fig. 2 shows that both calculations can reproduce the missing intensity into low-lying levels, as well as the strong population of a level around 4 MeV, although both overpredict its intensity. In addition, the large fragmentation of the experimental  $\beta$ -decay intensity at high energies is qualitatively reproduced by the shell-model calculation, but not with the QRPA one. QRPA calculations were also performed for various deformation parameters (inset of Fig. 2). It can be seen that the energy of the strongly populated level is changing with deformation, but the overall shape of  $I_\beta$  does not change significantly.

The extracted  $\beta$ -decay intensity was also used to calculate the  $\log(ft)$  values [51] and from that the Gamow-Teller strength distribution  $B(\text{GT})$  [27]. The cumulative  $B(\text{GT})$  for energies up to 10 MeV is shown in Fig. 3. The experimental values are shown as the solid black line with uncertainties indicated by the green-shaded area. The same theoretical calculations shown in Fig. 2 are also shown in Fig. 3 in the same line style. The theoretical calculations are missing significant strength at high energies, compared to the experimental results. For a better overview, the full range of the shell-model calculation, including the giant Gamow-Teller resonance, is shown in the inset of Fig. 3, renormalized by a quenching factor of 0.55 [52]. Beta decay to the  $^{70}\text{Ni}$   $0^+$  ground state would go by the  $\nu 0g_{9/2}$  to  $\pi 0f_{7/2}$  transition to the  $C(\nu 0g_{9/2})^2$  state, resulting in a fifth-forbidden  $\Delta J = 6^-$  type of  $\beta$  decay. The first Gamow-Teller strength around 3 MeV is dominated by the  $\nu 0f_{5/2}$  to  $\pi 0f_{7/2}$  transition to  $C(\nu 0f_{5/2})^{-1}(\nu 0g_{9/2})^3$  states. The

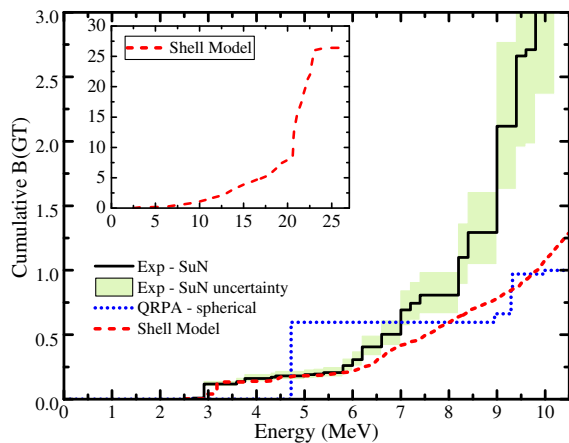


FIG. 3. Cumulative  $B(\text{GT})$  of  $^{70}\text{Co}$  versus excitation energy of the final states in  $^{70}\text{Ni}$ . The solid black line and green-shaded area are the experimental results with uncertainties. The dotted blue line is a QRPA calculation under the assumption of spherical shape. The dashed red line is a shell-model calculations (see the text for details). The inset presents the full spectrum of the shell-model calculation, including a quenching factor of 0.55, where the giant Gamow-Teller resonance can be observed around 23 MeV.

gradual rise starting at 5 MeV is dominated by  $\nu 0p$  to  $\pi 0p$ ,  $\nu 0f_{5/2}$  to  $\pi 0f_{5/2}$ , and  $\nu 0g_{9/2}$  to  $\pi 0g_{9/2}$ , leading to proton particle-hole states in  $^{70}\text{Ni}$ . The peak near 23 MeV is the giant Gamow-Teller resonance that is dominated by  $\nu 0f_{7/2}$  to  $\pi 0f_{5/2}$  and  $\nu 0g_{9/2}$  to  $\pi 0g_{7/2}$  transitions. The giant Gamow-Teller removes strength from the low energy states. The experimental strength above 6 MeV is about a factor of 2 larger than that calculated. This could be due to the spreading width of the higher state coming from mixing with  $2p - 2h$  configurations that are not in the calculation.

For the QRPA calculation, there may be additional factors that contribute to the missing strength observed in Fig. 3. On one hand, the present calculation does not include first-forbidden transitions, an effect that was shown to have significant impact on the distribution for spherical nuclei [53]. In addition, the Gamow-Teller residual interaction may be too strong due to the model assumption that the shapes of the mother and daughter nuclei are identical. It should be noted that while the QRPA  $\beta$ -decay intensity and  $B(\text{GT})$  shown in Figs. 2 and 3 are not in very good agreement with the data, the extracted half-life of 103.5 ms is in excellent agreement with the literature value.

To investigate further the competition between  $\gamma$  deexcitation and neutron emission above the neutron-separation energy, an additional calculation was performed, which calculates the  $\beta$ -delayed neutron-emission probability using the experimental  $\beta$ -decay intensity, based on the model assumptions presented in Ref. [54]. The calculated  $P_n$  value is 12.6%, which shows that above the neutron-separation energy, the emission of neutrons is assumed to dominate over  $\gamma$  emission. This in contrast to the observed  $\gamma$  emission from states all the way up to 10 MeV.  $\gamma$  emission from states above the neutron-separation energy has been observed in the past in the decay of  $^{137}\text{I}$  [55] and in the mass region around  $A = 90$  [56,57], although in both cases the effect does not extend more than a few hundred keV from the neutron threshold. In both cases, the neutron-emission hindrance was attributed to the large angular momentum difference between initial and final states. In Ref. [57], an increase in the  $\gamma$ -ray strength function is proposed to reproduce the neutron- $\gamma$  competition. In the present work, the  $P_n$  value calculation mentioned above [54] does include angular momentum considerations, assuming the uncertain spin assignments from Ref. [58]. In an effort to understand the additional hindrance of neutron emission, we used the shell-model calculation to examine the spectroscopic overlap between states above the neutron-separation energy and the low-lying states in  $^{69}\text{Ni}$ . Within the model truncations discussed above, we found that, on average, the spectroscopic factor was of the order of  $10^{-6}$ , which is not surprising since, as mentioned earlier, the relevant states in  $^{70}\text{Ni}$  include proton excitations and the low-lying states in  $^{69}\text{Ni}$  do not. This extremely small spectroscopic overlap can explain the reduction in neutron emission and the strong  $\gamma$  emission above the neutron threshold. Similar

conclusions were drawn in the recent work of Dungan *et al.* [59], in a different case of  $\gamma$ -neutron competition in  $^{19}\text{O}$ , from states populated in a transfer reaction. We therefore conclude that in the decay of neutron-rich nuclei, the neutron emission can be hindered due to the small spectroscopic overlap of the involved states, with a major impact on the calculated neutron-emission probability. An investigation of all nuclei where this effect may be important and the impact on  $r$ -process nucleosynthesis is currently in progress.

In summary, the present Letter reports on the first measurement of the  $\beta$ -decay intensity from the decay of  $^{70}\text{Co}$ . This nucleus offered the rare opportunity to study this quantity far from stability and within a broad energy range. We observed a surprisingly large fragmentation of the  $\beta$ -decay intensity at high energies, which is not well reproduced by the QRPA calculation, but in good qualitative agreement with the shell-model calculation. In addition, we observed an unexpectedly strong  $\gamma$  emission from levels above the neutron-separation energy. This was attributed to the very small spectroscopic overlap between populated states in  $^{70}\text{Ni}$  and low-lying states in the  $1n$  daughter  $^{69}\text{Ni}$ . Future work will investigate the presence of such  $\gamma$ - $n$  competition in other nuclei and the possible impact on  $r$ -process nucleosynthesis calculations.

We would like to thank R. G. T. Zegers for useful discussions. We gratefully acknowledge the support of NSCL operations staff. Financial support from the Research Council of Norway, Project Grant No. 205528 (A. C. L. and M. G.) and Project Grant No. 210007 (L. C. C., T. R., and S. S.) is gratefully acknowledged. A. C. L. acknowledges funding through the ERC-STG-2014 under Grant Agreement No. 637686. D. L. B. acknowledges the support of LLNL under Contract No. DE-AC52-07NA27344. The LANL work was carried out under the auspices of the NNSA of the U.S. Department of Energy at Los Alamos National Laboratory under Contract No. DE-AC52-06NA25396. This work was supported by the National Science Foundation under Grants No. PHY 1102511 (NSCL), No. PHY 1404442, No. PHY 0822648 (Joint Institute for Nuclear Astrophysics), and No. PHY 1350234 (CAREER). This work was also supported by NNSA Grants No. DE-NA-0000979 and No. DE-NA-0002132.

---

\*spyrou@nscl.msu.edu

- [1] K. M. Burbidge, G. R. Burbidge, W. A. Fowler, and F. Hoyle, *Rev. Mod. Phys.* **29**, 547 (1957).
- [2] A. G. W. Cameron, *Publ. Astron. Soc. Pac.* **69**, 201 (1957).
- [3] M. Arnould, S. Goriely, and K. Takahashi, *Phys. Rep.* **450**, 97 (2007).
- [4] C. Sneden, J. J. Cowan, and R. Gallino, *Annu. Rev. Astron. Astrophys.* **46**, 241 (2008).
- [5] S. Woosley, J. Wilson, G. Mathews, R. Hoffman, and B. Meyer, *Astrophys. J.* **433**, 229 (1994).
- [6] L. Hüdepohl, B. Müller, H.-T. Janka, A. Marek, and G. G. Raffelt, *Phys. Rev. Lett.* **104**, 251101 (2010).
- [7] T. Fischer, S. Whitehouse, A. Mezzacappa, F.-K. Thielemann, and M. Liebendörfer, *Astron. Astrophys.* **517**, A80 (2010).
- [8] G. Martínez-Pinedo, T. Fischer, A. Lohs, and L. Huther, *Phys. Rev. Lett.* **109**, 251104 (2012).
- [9] S. Wanajo, Y. Sekiguchi, N. Nishimura, K. Kiuchi, K. Kyutoku, and M. Shibata, *Astrophys. J.* **789**, L39 (2014).
- [10] O. Just, A. Bauswein, R. Pulpillo, S. Goriely, and H.-T. Janka, *Mon. Not. R. Astron. Soc.* **448**, 541 (2015).
- [11] A. Ji, A. Frebel, A. Chiti, and J. Simon, *Nature (London)* **531**, 610 (2016).
- [12] I. Roederer, J. Cowan, A. Karakas, K.-L. Kratz, M. Lugaro, J. Simmerer, K. Farouqi, and C. Sneden, *Astrophys. J.* **724**, 975 (2010).
- [13] M. Mumpower, R. Surman, G. C. McLaughling, and A. Aprahamian, *Prog. Part. Nucl. Phys.* **86**, 86 (2016).
- [14] D. Martin, A. Arcones, W. Nazarewicz, and E. Olsen, *Phys. Rev. Lett.* **116**, 121101 (2016).
- [15] P. Hosmer, H. Schatz, A. Aprahamian, O. Arndt, R. R. C. Clement, A. Estrade, K. Farouqia, K.-L. Kratz, S. N. Liddick, A. F. Lisetskiy *et al.*, *Phys. Rev. C* **82**, 025806 (2010).
- [16] J. V. Schelt *et al.*, *Phys. Rev. Lett.* **111**, 061102 (2013).
- [17] G. Lorusso *et al.*, *Phys. Rev. Lett.* **114**, 192501 (2015).
- [18] C. Forssen, F. S. Dietrich, J. Escher, R. D. Hoffman, and K. Kelley, *Phys. Rev. C* **75**, 055807 (2007).
- [19] J. Cizewski, R. Hatarik, K. Jones, S. Pain, J. Thomas, M. Johnson, D. Bardayan, J. Blackmon, M. Smith, and R. Kozub, *Nucl. Instrum. Methods Phys. Res., Sect. B* **261**, 938 (2007).
- [20] H. Utsunomiya, S. Goriely, H. Akimune, H. Harada, F. Kitatani, S. Goko, H. Toyokawa, K. Yamada, T. Kondo, O. Itoh *et al.*, *Phys. Rev. C* **82**, 064610 (2010).
- [21] J. E. Escher, J. T. Burke, F. S. Dietrich, I. J. T. N. D. Scielzo, and W. Younes, *Rev. Mod. Phys.* **84**, 353 (2012).
- [22] A. Spyrou, S. Liddick, A. Larsen, M. Guttormsen, K. Cooper, A. Dombos, D. Morrissey, F. Naqvi, G. Perdikakis, S. Quinn *et al.*, *Phys. Rev. Lett.* **113**, 232502 (2014).
- [23] J. Krumlinde and P. Möller, *Nucl. Phys.* **A417**, 419 (1984).
- [24] P. Möller, J. Nix, W. Myers, and W. Swiatecki, *At. Data Nucl. Data Tables* **59**, 185 (1995).
- [25] P. Möller, J. Nix, and K.-L. Kratz, *At. Data Nucl. Data Tables* **66**, 131 (1997).
- [26] B. Rubio, W. Gelletly, E. Náchter, A. Algora, J. Taín, A. Pérez, and L. Caballero, *J. Phys. G* **31**, S1477 (2005).
- [27] Y. Fujita, B. Rubio, and W. Gelletly, *Prog. Part. Nucl. Phys.* **66**, 549 (2011).
- [28] M. Wang, G. Audi, A. Wapstra, F. Kondev, M. MacCormick, X. Xu, and B. Pfeiffer, *Chin. Phys. C* **36**, 1603 (2012).
- [29] P. Möller, A. Sierk, T. Ichikawa, and H. Sagawa, *At. Data Nucl. Data Tables* **109-110**, 1 (2016).
- [30] J. Wood, K. Heyde, W. Nazarewicz, M. Huyse, and P. van Duppen, *Phys. Rep.* **215**, 101 (1992).
- [31] S. Liddick, S. Suchyta *et al.*, *Phys. Rev. C* **84**, 061305 (2011).
- [32] M. P. Carpenter, R. V. F. Janssens, and S. Zhu, *Phys. Rev. C* **87**, 041305 (2013).

- [33] S. Suchyta, S. Liddick, Y. Tsunoda, T. Otsuka, M. Bennett, A. Chemey, M. Honma, N. Larson, C. Prokop, S. Quinn *et al.*, *Phys. Rev. C* **89**, 021301(R) (2014).
- [34] C. J. Prokop, B. P. Crider, S. N. Liddick, A. D. Ayangeakaa, M. P. Carpenter, J. J. Carroll, J. Chen, C. J. Chiara, H. M. David, A. C. Dombos *et al.*, *Phys. Rev. C* **92**, 061302 (2015).
- [35] C. Chiara *et al.*, *Phys. Rev. C* **91**, 044309 (2015).
- [36] R. Grzywacz *et al.*, *Phys. Rev. Lett.* **81**, 766 (1998).
- [37] W. Mueller *et al.*, *Phys. Rev. C* **61**, 054308 (2000).
- [38] O. Sorlin, C. Donzaud *et al.*, *Nucl. Phys.* **A719**, C193 (2003).
- [39] M. Sawicka *et al.*, *Phys. Rev. C* **68**, 044304 (2003).
- [40] D. J. Morrissey, B. Sherrill, M. Steiner, A. Stolz, and I. Wiedenhoever, *Nucl. Instrum. Methods Phys. Res., Sect. B* **204**, 90 (2003).
- [41] S. Liddick, A. Spyrou, B. Crider, F. Naqvi, A. C. Larsen, M. Guttormsen, M. Mumpower, R. Surman, G. Perdikakis, D. Bleuel *et al.*, *Phys. Rev. Lett.* **116**, 242502 (2016).
- [42] A. Simon, S. Quinn, A. Spyrou *et al.*, *Nucl. Instrum. Methods Phys. Res., Sect. A* **703**, 16 (2013).
- [43] J. C. Hardy, L. C. Carraz, B. Jonson, and P. G. Hanse, *Phys. Lett.* **71B**, 307 (1977).
- [44] T. Kurtukian-Nieto, J. Benlliure, and K.-H. Schmidt, *Nucl. Instrum. Methods Phys. Res., Sect. A* **589**, 472 (2008).
- [45] A. Morales, J. Benlliure, M. Górska, H. Grawe, S. Verma, P. Regan, Z. Podolyák, S. Pietri, R. Kumar, E. Casarejos *et al.*, *Phys. Rev. C* **88**, 014319 (2013).
- [46] F. Bečvář, *Nucl. Instrum. Methods Phys. Res., Sect. A* **417**, 434 (1998).
- [47] C. Prokop, Ph.D. thesis, Michigan State University (2016), [https://publications.nsl.msu.edu/thesis/Prokop2016\\_401.pdf](https://publications.nsl.msu.edu/thesis/Prokop2016_401.pdf).
- [48] M. Honma, T. Otsuka, B. A. Brown, and T. Mizusaki, *Phys. Rev. C* **69**, 034335 (2004).
- [49] D. R. Entem and R. Machleidt, *Phys. Rev. C* **68**, 041001(R) (2003).
- [50] <https://github.com/ManyBodyPhysics/CENS>.
- [51] National Nuclear Data Center, [www.nndc.bnl.gov/logft](http://www.nndc.bnl.gov/logft).
- [52] G. Martínez-Pinedo, A. Poves, E. Caurier, and A. P. Zuker, *Phys. Rev. C* **53**, 2602(R) (1996).
- [53] P. Moller, B. Pfeiffer, and K.-L. Kratz, *Phys. Rev. C* **67**, 055802 (2003).
- [54] T. Kawano, P. Möller, and W. B. Wilson, *Phys. Rev. C* **78**, 054601 (2008).
- [55] H. Ohm, M. Zendel, S. Prussin, W. Rudolph, A. Schröder, K.-L. Kratz, C. Ristori, J. Pinston, E. Monnard, F. Schussler *et al.*, *Z. Phys. A* **296**, 23 (1980).
- [56] S. Raman, B. Fogelberg, J. A. Harvey, R. L. Macklin, P. H. Stelson, A. Schroder, and K.-L. Kratz, *Phys. Rev. C* **28**, 602 (1983).
- [57] J. Tain *et al.*, *Phys. Rev. Lett.* **115**, 062502 (2015).
- [58] National Nuclear Data Center, Evaluated Nuclear Structure Data File (ENSDF) Retrieval, [www.nndc.bnl.gov](http://www.nndc.bnl.gov).
- [59] R. Dungan, S. L. Tabor, V. Tripathi, A. Volya, K. Kravvaris, B. Abromeit, D. D. Caussyn, S. Morrow, J. J. Parker IV, P.-L. Tai *et al.*, *Phys. Rev. C* **93**, 021302(R) (2016).